Journal of Statistical Physics, Vol. 80, Nos. 3/4, 1995

Velocity Autocorrelation Function in Lattice Gases from the Ring Kinetic Theory. Comparison with Numerical Simulations

R. Brito[1,2] and G. A. van Velzen[3]

Received December 5, 1994; final January 30, 1995

We obtain the complete time dependence of the velocity autocorrelation function (VACF) for lattice gas cellular automata, using *ring kinetic theory*. This theory accounts for the simplest correlated collisions that improve on the molecular chaos approach, and yields a closed equation for the VACF that we evaluate for both infinite and finite systems. We compare our analytical results with numerical simulations at all times, as well as with long-time results of the mode coupling theories, finding a very good agreement for all times at all densities.

KEY WORDS: Lattice gas automata; velocity autocorrelation function; diffusion coefficient; ring collisions.

1. INTRODUCTION

The velocity autocorrelation function (VACF) of a tagged particle plays a fundamental role in the theory of nonequilibrium processes. It describes the time decay of the velocity of a tagged particle in a fluid. The time integral of the VACF gives the self-diffusion coefficient, through a Green–Kubo relation.[1] Furthermore, it is possible to relate quantities in nonequilibrium with correlation functions in equilibrium, like the VACF, via the Onsager hypothesis. It was believed, based on the Boltzmann approximation, that the VACF had an exponential decay in time. This is indeed the case for

[1] Institute for Theoretical Physics, University of Utrecht, P.O.B. 80006, 3508 TA Utrecht, The Netherlands.

[2] Permanent address: Facultad de Ciencias Físicas, Universidad Complutense de Madrid, 28040-Madrid, Spain.

[3] Physical Planning Division, Grontmij Consulting Engineers, P.O.B. 203, 3730 AE De Bilt, The Netherlands.

0022-4715/95/0800-0565$07.50/0

short times, where the Boltzmann approximation is valid. However, numerical simulations for hard spheres[2] showed that the time decay was not exponential but algebraic, of the form $t^{-d/2}$, where d is the dimensionality of the system. Phenomenological explanation to this result was given by the mode coupling theory,[3] which applies only for long times.

Lattice gas automata (LGA)[4] are suitable models to study these phenomena because their simplicity makes it possible to carry out a theoretical analysis. They are discrete models created to obtain solutions of the Navier–Stokes equations.[5] As they behave at the level of the Navier–Stokes equations as real fluids, information from their VACF can be extrapolated to real fluids, in particular the long-time behavior. An important feature in this context is that the VACF in LGA can be simulated with very high statistical accuracy using the so-called *moment propagation method*,[6,7] which is an exact algorithm of enumeration of all possible trajectories of a tagged particle, given an initial configuration. At long times the simulations show an excellent agreement with the algebraic decay given by the mode coupling results[8] for two-, three-, and four-dimensional systems.[7,9,10] Furthermore, the mode coupling theory has been adapted to LGA in *finite* systems,[11,12] following the lines of ref. 13, by taking into account the contribution of sound modes and the finite set of allowed wave vectors. Again, the comparison with numerical simulations shows a very good agreement.

In this paper we deal with the full time dependence of the VACF. In particular, we are interested in the crossover from the exponential regime (valid for short times) to the algebraic one (applicable for long times). These two regimes are well known and checked against numerical simulations. Furthermore, we will study the effects caused by finite system sizes. We use the recenty developed ring kinetic theory for lattice gases[14] in its version for the tagged particle problems.[15] This theory only takes into account the simplest correlated ring collisions, yielding a closed expression for the VACF at all times (repeated ring theory or self-consistent ring theory will not be considered). We evaluate this expression, and show that only with this type of collision is it possible to give a very accurate answer for the VACF at all times, for both finite and infinite systems. The ring kinetic theory has been successfully applied to evaluate transport coefficients,[16] providing very good results: the difference from the simulated transport coefficients is less than 5% (the Boltzmann approximation has deviations of around 20%).

The plan of this paper is as follows. Section 2 recalls some definitions and general results about LGA, as well as the calculation of the VACF in the Boltzmann approximation. In the following section a brief summary of the ring kinetic theory is presented. In Section 4 we present the results

obtained with such theory for both infinite system size and for finite system size, comparing them with the available numerical simulations as well as with the results from mode coupling theory.

2. LATTICE GASES

Lattice gases are systems in which both space and time are discrete. There are N particles, with positions belonging to the nodes of a d-dimensional regular lattice $\mathscr{L}$. At integer times, particles jump from one node to another, according to their velocities. Hence the nonzero velocities have unit size and discrete directions: $\mathbf{c}_i$, $i=1,\ldots, b$, where b is called "number of bits." The set of allowed velocities usually coincides with the set of nearest-neighbor vectors, and possibly there is a rest particle with $\mathbf{c}_i=0$. The state of a LGA is fully described by giving the occupation numbers $\{n_i(\mathbf{r}, t),\ \mathbf{r}\in\mathscr{L},\ i=1,\ldots, b\}$, which take the value 1 if there is a particle at node $\mathbf{r}$ with velocity $\mathbf{c}_i$ at time t, and 0 otherwise.

The time evolution of a LGA consists of two steps: collision and propagation. First the collision step is performed according to certain collision rules that conserve number and total momentum at each node. They are specified in the collision operator $I(n)$, which is a nonlinear function of the occupation numbers n_i, in general a polynomial of degree b. After the collision step has taken place, the propagation is performed simply by moving a particle from node $\mathbf{r}$ to node $\mathbf{r}+\mathbf{c}_i$, where $\mathbf{c}_i$ is the velocity of the particle. Combination of collision and propagation gives the evolution equation for the occupation numbers:

$$n_i(\mathbf{r}+\mathbf{c}_i, t+1)=n_i(\mathbf{r}, t)+I_i[n(t)] \tag{2.1}$$

The first term on the right-hand side of this equation represents the propagation step, and the second term accounts for the collisions. If f denotes the equilibrium average occupation number $f=\langle n_i(\mathbf{r}, t)\rangle$, we can expand the collision operator in terms of fluctuations as

$$I_i[n]=\sum_{\lambda=1}^{b}\frac{1}{\lambda!}\,\Omega^{(\lambda)}_{ii_1\cdots i_\lambda}\,\delta n_{i_1}\cdots\delta n_{i_\lambda}\equiv\Omega^{(1)}_{ii_1}\,\delta n_{i_1}+\Omega_i[n(t)] \tag{2.2}$$

where the fluctuations in the occupation numbers are $\delta n_i(\mathbf{r}, t)=n_i(\mathbf{r}, t)-f$. The equilibrium relation $I_i(f)=0$ has been used in (2.2). Some properties of the $\Omega^{(\lambda)}$ coefficients can be found in the literature.[15]

In order to study the VACF we need to tag one of the fluid particles and register its trajectory. Furthermore, we have to specify the collision rules between the tagged particle and the fluid particles. There are many

ways to choose such rules,[17] but we will consider the so-called *maximally random collision rules*, in which the tag is redistributed randomly among the particles present at a node, regardless of whether a collision has taken place or not. These are the collision rules used in the numerical simulations[6,7] that we will compare with. For the tagged particle there is a dynamical equation equivalent to (2.1), but with n replaced by $\bar{n}$ (which is the occupation number of the tagged particle). Also, we define $\bar{I}$ and $\bar{\Omega}$ through an equation similar to (2.2) for tagged particles. In terms of these occupation numbers, the velocity of a tagged particle is simply $\mathbf{v}(t) = \sum_{\mathbf{r},i} \mathbf{c}_i \bar{n}_i(\mathbf{r}, t)$.

The ring kinetic theory is formulated in terms of the kinetic propagator $\bar{\Gamma}$, defined as

$$\bar{\Gamma}_{ij}(\mathbf{r}, t) = bV\langle \delta\bar{n}_i(\mathbf{r}, t)\, \delta\bar{n}_j(0, 0)\rangle \tag{2.3}$$

where V is the number of sites of the lattice. The kinetic propagator is a correlation function evaluated at equilibrium (i.e., $\langle \cdots \rangle$ is an average over an equilibrium ensemble). In terms of $\bar{\Gamma}$, the VACF $\phi(t)$ is defined as

$$\phi(t) = V \sum_{\mathbf{r},ij} c_{ix} c_{jx} \langle \bar{n}_i(\mathbf{r}, t)\, \bar{n}_j(0, 0)\rangle = \frac{1}{b} \sum_{\mathbf{r},ij} c_{ix} c_{jx} \bar{\Gamma}_{ij}(\mathbf{r}, t) \tag{2.4}$$

and the diffusion coefficient by a Green–Kubo formula,[18] i.e., by the time sum of $\phi(t)$, where the $t = 0$ term only counts half due to the discreteness of time:

$$D = \sum_{t=1}^{\infty} \phi_x(t) + \tfrac{1}{2}\phi_x(0) \tag{2.5}$$

Prior to the ring kinetic theory, the diffusion coefficient had been only evaluated in the Boltzmann approximation, based on the molecular chaos assumption in which sequences of correlated collisions are neglected.[19] This approximation is simply obtained by keeping in (2.2) only the linear term in δn, related with $\Omega^{(1)}_{ij}$. Then the kinetic propagator is reduced to

$$\bar{\Gamma}^{\mathrm{B}}_{ij} = [S^{-1}(\mathbb{1} + \bar{\Omega}^{(1)})]^t_{ij} \tag{2.6}$$

Furthermore, for most of the existing LGA, one can prove that $\mathbf{c}$ is an eigenvector of $\Omega^{(1)}$ with eigenvalue $-\omega$. In this case, simple algebra shows[17]

$$\phi_{\mathrm{B}}(t) = \phi(0)(1 - \omega)^t \tag{2.7}$$

that is, an *exponential* decay of $\phi(t)$. For the case of maximally random collision rules, ω only depends on the density f and the number of bits b, but not on the detailed collision rules.[17] The value of ω is then

$$1-\omega=\frac{1-f}{(b-1)f}[1-(1-f)^{b-1}] \tag{2.8}$$

Although the value for the diffusion coefficient given by the Boltzmann approximation [obtained using (2.5), (2.7), and (2.8)] differs less than 1% from the simulations,[7] the qualitative behavior is wrong. Boltzmann predicts an exponential VACF for all times, as shown in Eq. (2.7), while the correct one for long times is algebraic, as predicted by mode coupling theory and shown in the simulations (see, however, next section).

3. RING THEORY FOR VELOCITY AUTOCORRELATION FUNCTION

The ring kinetic theory improves on the Boltzmann approximation by considering the simplest correlated collisions. These collisions consist of two particles colliding at a certain point at a certain time. Then they propagate independently, eventually colliding with other particles. Finally the two particles meet again, closing the *correlated* collision. The mathematical structure of such collisions will be made clear in this section. Here we summarize the results of the ring kinetic theory for the VACF presented in ref. 15, where a detailed description of this theory can be found. The ring theory gives an approximate closed expression for the propagator in Fourier space. In the cases described in Section 2, where $\mathbf{c}$ is an eigenvector of $\bar{\Omega}^{(1)}$, it can be simplified to

$$\phi(t)=\phi_{\mathrm{B}}(t)+b^{-1}\sum_{\tau=1}^{t-1}\tau(1-\omega)^{\tau-1}A_{x,ij}R_{ij,kl}(t-\tau-1)A_{x,kl} \tag{3.1}$$

where $A_{x,ij}$ is the x-component of

$$\mathbf{A}_{ij}=\sum_k \mathbf{c}_k\bar{\Omega}^{(2)}_{kij} \tag{3.2}$$

The coefficients $\bar{\Omega}^{(2)}_{ijk}$ are the quadratic terms in the fluctuation expansion of the tagged particle collision operator. They are the equivalent of (2.2) for tagged particles. The values of the coefficients $\mathbf{A}_{ij}$ are independent of the particular set of collision rules chosen, as it happened with the eigenvalue ω.

They can be found in ref. 15. In the expression for the VACF (3.1), we have used the *ring operator*, defined as

$$R_{i_1 i_2, j_1 j_2}(\mathbf{k}, \tau) = \frac{f(1-f)}{V} \sum_{\mathbf{q}} \bar{\Gamma}^{\mathrm{B}}_{i_1 j_1}(\mathbf{q}, \tau)\, S^{-1}_{j_1}(\mathbf{q})\, \Gamma^{\mathrm{B}}_{i_2 j_2}(\mathbf{k}-\mathbf{q}, \tau)\, S^{-1}_{j_2}(\mathbf{k}-\mathbf{q}) \tag{3.3}$$

where the sum over $\mathbf{q}$ vectors is restricted to the set of reciprocal lattice vectors. Furthermore, Γ^{B} is the kinetic propagator of a fluid particle in the Boltzmann approximation [i.e., Eq. (2.6) with $\bar{\Omega}^{(1)}$ replaced by $\Omega^{(1)}$] and S is the translation operator: $S = \exp(i\mathbf{q} \cdot \mathbf{c}_i)$.

The ring term in Eq. (3.1) has the normal structure of the ring collision term in the kinetic theory of continuum fluids.[20] It consists of three terms: a binary collision which is the origin of the correlated collision, accounted for by $A_{x,ij}$; then two particles propagating independently, given by two parallel propagators included in $R_{ij,kl}(t-\tau-1)$; finally, a recollision of the two particles contributing with $A_{x,kl}$.

The ring theory, as expressed in Eq. (3.1) gives in the long-time limit the so-called full mode coupling theory.[15] This is a mode coupling theory in which all possible pairs of modes are included (both sound modes and shear modes) and the discreteness of the $\mathbf{q}$-sum is maintained, so finite-size effects are taken into account in a straightforward manner.[13] The full mode coupling theory (and consequently the ring kinetic theory) shows very good agreement with the numerical simulations for intermediate and long times for the FHP-III model.[11] As the system size grows, the $\mathbf{q}$ spacing is reduced, and the $\mathbf{q}$-sum can be replaced by an integral over the first Brillouin zone. Furthermore, if only the contributions from pairs of shear modes are taken (which is the dominant part), the VACF for FHP models reduces to

$$\phi(t) = \frac{(1-f)\sqrt{3}}{16bf} \frac{1}{(\nu + D)\, t} \tag{3.4}$$

where ν is the shear viscosity. We refer to this result as the asymptotic long-time tail. The onset time for this regime is some $10t_{\mathrm{mf}}$, where t_{mf} is the time between collisions. It is given by $t_{\mathrm{mf}} = -1/\ln(1-\omega)$, and ω is defined in Eq. (2.8). In two-dimensional systems, however, Eq. (3.4) leads to an inconsistency. The diffusion coefficient is obtained as the time integral of $\phi(t)$ as $t \to \infty$, with the result that $D \to \infty$ as $t \to \infty$, making Eq. (3.4) meaningless. This is also the case for the shear viscosity ν. In order to solve this problem, Wainwright *et al.*[21] introduced a *self-consistent* mode coupling theory, where transport coefficients in Eq. (2.8) depend on time. This yields a self-consistent equation that, when solved, shows that the decay of $\phi(t)$

is no longer algebraic, but proportional to $\{t[\log(t/t_s)]^{1/2}\}^{-1}$, slightly faster than t^{-1}. This is called the super-long-time regime. There is numerical evidence of the $\{t[\log(t/t_s)]^{1/2}\}^{-1}$ decay.[22] However, as the time t_s is estimated to be some 10^{20} mean free times, the super-long-time regime is far from the actual computer power.

To summarize, the temporal behavior of the VACF is the following. First, for few mean free times the VACF shows an exponential decay as predicted by Eq. (2.7). At longer times (as will be discussed in the next section) the VACF is given by the full mode coupling theory, with sound modes included. The contribution of the sound modes decays faster than that of the shear modes, so at later times the asymptotic long-time tail [Eq. (3.4)] is reached. This is the final regime for systems of more than two spatial dimensions. For two-dimensional systems, after $10^{20}t_{mf}$ the super-long-time tail of the form $\{t[\log(t/\tau)]^{1/2}\}^{-1}$ is followed, which is the *true* asymptotic regime. However, for the system sizes and times considered in this paper, this super-long-time tail is not seen at all, at most of the simulations show.[7,9,10] As mentioned in the introduction, we are mainly interested in the crossover from the Boltzmann regime to the algebraic long-time tails, where no theoretical results are available so far. The ring kinetic theory attempts to fill this gap and supply such theoretical values for the VACF in the intermediate-time regime.

In the case of *finite* systems there is a correction to the VACF of $\mathcal{O}(1/N)$ due to the finite number of particles in the system. This contribution was analyzed for classical fluids in ref. 13 and for lattice gases in ref. 11. Its value in the latter case is given by $(1-f)/N$ [it is the $\mathbf{q}=0$ term in Eq. (3.3)]. From here on we will use the corrected VACF, denoted by $\psi(t)$, in order to compare with the infinite-size results, i.e., $\psi(t)=\phi(t)+(1-f)/N$.

4. RESULTS

In this section we present the results of the numerical integration of Eq. (3.1) and its comparison with the available numerical data for the so-called FHP-III, a seven-bit model defined on a triangular lattice, with up to six moving and one rest particle per site.[23] We will compare our results with the full mode coupling theory and with the asymptotic long-time tail, as given in Eq. (3.4).

4.1. Infinite Systems

For infinite systems, the finite $\mathbf{q}$-sum in (3.3) can be replaced by an integration over the first Brillouin zone,

$$V^{-1}\sum_{\mathbf{q}} \to \frac{v_0}{(2\pi)^d}\int_{1BZ}$$

where v_0 is the volume of the unit cell ($v_0 = \sqrt{3}/2$ for the triangular lattice). We perform this integral following a Gaussian integration procedure, as explained in ref. 16. We plot in Figs. 1 and 2 the decimal logarithm of the VACF $\phi(t)$ versus the decimal logarithm of time t. It is normalized to $\phi(0) = 1$. We recall that for infinite systems there is no distinction between the corrected and uncorrected VACF [$\psi(t)$ and $\phi(t)$]. We present the results of ring kinetic theory (solid line) together with the numerical simulations (crosses). We also plot results of the full mode coupling theory (dotted line) and the asymptotic long-time Eq. (3.4) (dashed-dotted line). Furthermore, the long-dashed line is the exponential decay according to the Boltzmann approach, Eq. (2.7). The densities are $f = 0.25$ in Fig. 1 and $f = 0.8$ in Fig. 2. The numerical simulations have been done in systems with size $V = 500 \times 500$ for times $t \leqslant 100$. Thus, as the maximum time is $t = 100$, there are no correlations induced by the boundary, as will be discussed in the next section. Furthermore, the finite-size corrections are smaller than 2×10^{-6} and 2×10^{-7}, respectively. We see in these two figures that the ring theory gives excellent predictions for all times, as the solid line passes almost through the simulation points.

We can analyze the results in terms of the mean free time t_{mf}, the average time between collisions, given by $t_{mf} = -1/\ln(1-\omega)$. The values of t_{mf} are $t_{mf} = 1.1$ for $f = 0.25$ and $t_{mf} = 0.3$ for $f = 0.8$. For short times, $t \lesssim 5t_{mf}$, the VACF is dominated by the Boltzmann value, Eq. (2.7), plotted in Fig. 1 with a long-dashed line. The higher the density, the shorter t_{mf}, as in Fig. 2, where the Boltzmann regime lasts only for two time steps [the Boltzmann regime is always exact for $t \leqslant 2$, as can be seen from Eq. (3.1)]. Only after this initial period do sequences of correlated collisions start to appear, producing deviations from the Boltzmann value.

After $10t_{mf}$ the VACF is dominated by the full mode coupling contribution as seen in these figures. However, there is a crossover from the full mode coupling (dotted line in the figures), where contributions coming from the fast-decaying sound modes are still important,[11] to the asymptotic long-time tail (dashed-dotted line), where only the shear modes survive. In this last case the VACF is given by Eq. (3.4). In order to check this result, we have fit the quantity $t\phi(t)$ to a constant, for the ring kinetic theory as well as the simulations results. The fits are done for times longer than $20t_{mf}$, up to $250t_{mf}$ in some cases. The simulation values have been obtained averaging over more than 100 realizations. We compare them with the results of the mode coupling theory, Eq. (3.4), where the transport coefficients ν and D have been replaced by their Boltzmann values. The

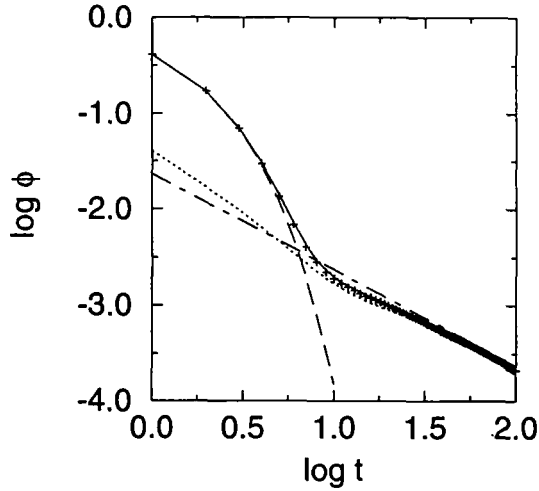

Fig. 1. Decimal logarithm of the velocity autocorrelation function vs. decimal logarithm of time t for the FHP-III model at density $f = 0.25$ and a system size of 500×500. The VACF is normalized such that $\phi(0) = 1$. Crosses are numerical simulations, and the solid line is the prediction of the ring theory. The dashed-dotted line represents the mode coupling theory with only shear contributions, while the dotted line is the result of the full mode coupling theory. The long-dashed line is the exponentially decaying VACF according to the Boltzmann approximation.

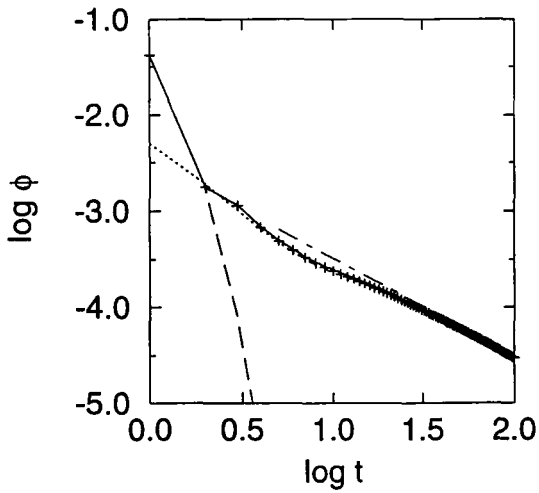

Fig. 2. The same as Fig. 1, for density $f = 0.8$.

Table I. Amplitudes of the Long-Time Tails in Infinite Systems as a Function of the Density[a]

Density	Ring	Simulation	Mode coupling
0.25	0.0231	0.0224 ± 0.0002	0.0234
0.40	0.0170	0.0163 ± 0.0001	0.0172
0.50	0.0129	0.0125 ± 0.0002	0.0132
0.60	0.00930	0.00877 ± 0.00007	0.00944
0.70	0.00596	0.00576 ± 0.00004	0.00610
0.80	0.00317	0.00300 ± 0.00003	0.00323

[a] The second column is the result of the ring kinetic theory. The third one corresponds to the numerical simulations with their error bars, averaged over 100 realizations. The last column is the result of the mode coupling theory, Eq. (3.4).

results are presented in Table I. We see that the results given by the ring kinetic theory agree very well with the asymptotic mode coupling result, as it should be, because the latter is an asymptotic limit of the former. The agreement with the numerical simulations is also very good, although the values do not coincide within the error bars. This is due to the fact that in the mode coupling result we have used the Boltzmann values for the transport coefficients. For the viscosity, they differ by about 20% with the simulated ones for the typical system sizes and times used in these simulations.[16,24] For the diffusion coefficients the difference is much smaller, about 1%.[9] When we use the real values for the transport coefficients, the amplitude of the long-time tail as given by the mode coupling result of Eq. (3.4) increases typically by a factor of 4–5%, improving the agreement with the numerical simulations.

Finally, in the intermediate-time regime (between $5t_{\text{mf}}$ and $10t_{\text{mf}}$) one could expect that more complicated recollisions (correlated collisions with more than two parallel propagators, rings within rings,...) would play an important role. However, as illustrated in Figs. 1 and 2, there is little room for contributions coming from these more complicated diagrams. Comparison of the simulation data with the numerical evaluation of the ring kinetic theory at intermediate times shows that the discrepancy is smaller than 5% at density $f = 0.25$ and smaller than 3% at $f = 0.8$. Along these lines, calculations for this model for the shear correlation function give that collisions with three or more parallel propagators add corrections smaller than 0.1% at time $t = 3$ for all densities.[16] Thus, the ring kinetic theory describes very well the complete time dependence of the VACF for infinite systems.

4.2. Finite Systems

Simulations are usually carried out in finite systems with periodic boundary conditions. When looking at long times, dynamic effects may have propagated from the basic cell to one of the neighboring replicas. These interference effects are caused mainly by traveling sound waves that cross the systems through the boundaries. The result is a net increase of the VACF because of the following mechanism. A tagged particle with velocity $\mathbf{v}$ gives part of its momentum to the surrounding fluid particles, which can create a sound wave with direction parallel to $\mathbf{v}$. This wave crosses the system through the boundary and hits the tagged particle from behind, producing a positive extra correlation between $\mathbf{v}(t)$ and $\mathbf{v}(0)$ that has to be added to the usual correlation between these two velocities.[25] The effect described would be the opposite in systems without periodic boundary conditions but with elastic walls: the sound wave could reverse its velocity after bounding off the wall, producing an extra negative correlation. These extra correlations produced in the system are *geometric* rather than dynamical; they are produced by the special (finite-size) geometry of the system and they are absent in infinite systems.

Because of the previous argument, the typical time in which the interference effects is produced is the time that a sound wave needs to cross the system, i.e., between L/c_0 (x-direction) and $\sqrt{3}L/2c_0$ (y-direction), where c_0 is the speed of sound ($c_0 = \sqrt{3/7} \simeq 0.65$ in our model) and L is the linear size of the system (for a more detailed analysis of the characteristic times, we refer to ref. 11). Strictly speaking, the effects of finite size can already be seen immediately after $t = L_m/2$ time steps (where L_m is the smallest periodicity of the system). This is so because it is the time that two particles traveling in opposite directions need to cross the system and produce extra correlations. However, this effect just after $t = L_m/2$ is tiny, although existent. Only when the collective motion is set (like a sound wave) is the contribution noticeable, as discussed in the previous paragraph. There is one case in which this discussion is not fully applicable. In the case of the projected FCHC model,[26] when $L_m = 2$, important geometric correlations have been observed after only two time steps in the simulations[9] and explained with the help of the ring kinetic theory.[27]

In order to evaluate the ring theory for finite systems with periodic boundary conditions, we keep the finite $\mathbf{q}$ sum in Eq. (3.3). The values of the reciprocal lattice vectors for a finite system are obtained by imposing the periodicity condition $e^{i\mathbf{q}\cdot(\mathbf{r}+\mathbf{L})} = e^{i\mathbf{q}\cdot\mathbf{r}}$, where $\mathbf{r}$ is any vector of the lattice and $\mathbf{L}$ determines the periodicity of the system. For a triangular lattice of size $L \times L$ these vectors are $\mathbf{q} = (n_1/L)\,\mathbf{q}_1 + (n_2/L)\,\mathbf{q}_2$, $n_1, n_2 = 0, \ldots, L-1$, where $\mathbf{q}_1 = 2\pi(-1, 1/\sqrt{3})$ and $\mathbf{q}_2 = 2\pi(0, 2/\sqrt{3})$ are the basis vectors of the reciprocal lattice.

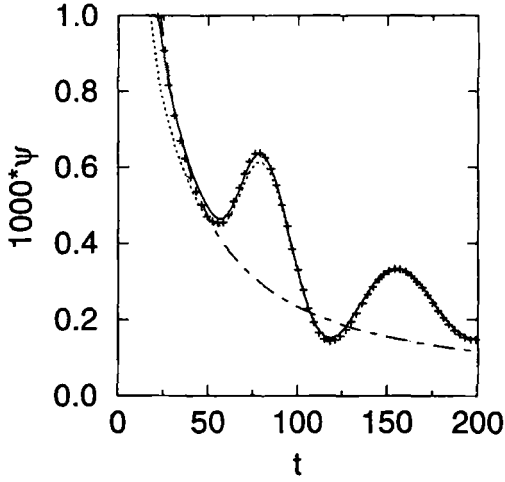

Fig. 3. Corrected velocity autocorrelation function at density $f = 0.2$ and system size 60×60. Lines are drawn as for Fig. 1.

Figure 3 shows the corrected VACF $\psi(t)$ as predicted by the ring kinetic theory (solid line) versus time, together with the numerical simulations (crosses) for a 60×60 system at density $f = 0.2$ (the mean free time is $t_{mf} \simeq 1.4$). The full mode coupling theory is plotted with a dotted line, and the asymptotic tail with a dotted-dashed line. It can be seen that the ring theory gives again excellent results with errors smaller at all times than 3% in Fig. 3 and 6% in Fig. 4. For times shorter than 50 time steps, the VACF approaches the asymptotic tail, because the system did not have time to create geometric correlations through the boundaries. The interference effects start at $t \simeq 50$, reaching the maximum at $t \simeq 80$ (in this case $\sqrt{3}L/2c_0 \simeq 78$) and decreasing again. The second maximum is produced at $t \simeq 160$ when the sound wave has crossed the system twice. This effect will continue creating more maxima in the VACF until it will finally reach the asymptotic state. In bigger systems the asymptotic regime is fully reached before the interference effects show up.

In order to see more clearly the difference between the data, we plot in Fig. 4 the corrected VACF $\psi(t)$ multiplied by time t vs. t, so the differences are magnified. This is a system at density $f = 0.5$ and system size $L = 50$. The asymptotic long-time tail is transformed into the horizontal dashed-dotted line. Here we can see that the asymptotic long-time regime is not fully reached before the interference with sound modes coming from the neighbor replicas appear. In this case, as the system is smaller than in Fig. 3, we can observe three maxima, around $t \simeq 70$, 130, 195 (for Fig. 3,

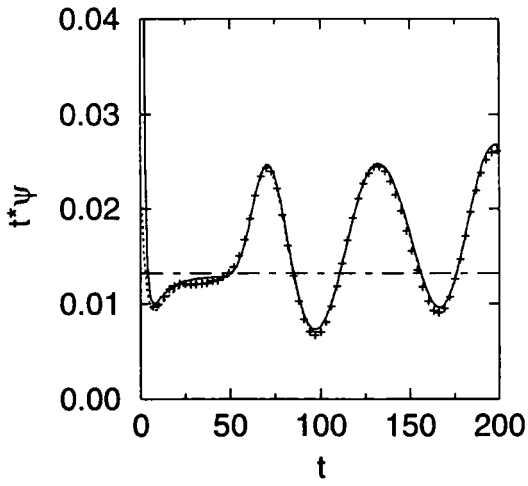

Fig. 4. Corrected velocity autocorrelation function multiplied by time t for density $f = 0.5$ and system size $L = 50$. Lines are drawn as for Fig. 1.

$\sqrt{3}L/2c_0 \simeq 67$). As we see, there is almost perfect agreement between the simulations and the ring theory, and also with the full mode coupling at long times.

5. CONCLUSIONS

We have presented in this paper the numerical evaluation of the ring kinetic theory applied to the velocity autocorrelation function in lattice gases. This theory only takes into account the simplest correlated event, two particles colliding at a point, propagating independently, and recolliding after a certain time. We have illustrated the results for both infinite and finite systems, showing excellent agreement with the numerical simulations. For infinite systems, the ring theory leads to the full mode coupling theory, showing the long-time tail t^{-1}. For finite systems, with interference effects coming from the periodic boundary conditions, the ring theory describes very accurately the values of the VACF. Furthermore, as can be seen in the figures, the ring kinetic theory agrees completely with the numerical data for *all* time regimes. Thus, the dynamics of the VACF in the lattice gas is dominated by the uncorrelated collisions (Boltzmann type) at short times, and beyond that, the only important type of collision seems to be that with two parallel propagators, the ring collision. More complicated sequences, such as rings within rings, rings with more parallel propagators, or other correlated collisions, are not important in the description of the VACF.

ACKNOWLEDGMENTS

The authors want to thank M. H. Ernst, H. J. Bussemaker, M. van der Hoef, D. Frenkel, and J. W. Dufty for many stimulating and clarifying discussions. R.B. acknowledges support by DGICYT (Spain) under contract number PB91-0378 and a grant of the Ministerio de Educación (Spain).

REFERENCES

1. J. Hansen and I. R. McDonald, *Theory of Simple Liquids*, 2nd ed. (Academic Press, London, 1986).
2. B. J. Alder and T. E. Wainwright, *Phys. Rev. A* **1**:18 (1970).
3. M. H. Ernst, E. Hauge, and J. M. J. van Leeuwen, *Phys. Rev. A* **4**:2055 (1971); *J. Stat. Phys.* **15**:7 (1976).
4. U. Frisch, B. Hasslacher, and Y. Pomeau, *Phys. Rev. Lett.* **56**:1505 (1986).
5. U. Frisch, D. d'Humières, B. Hasslacher, P. Lallemand, Y. Pomeau, and J. P. Rivet, *Complex Syst.* **1**:649 (1987).
6. D. Frenkel and M. H. Ernst, *Phys. Rev. Lett.* **63**:2165 (1989).
7. M. A. van der Hoef and D. Frenkel, *Phys. Rev. A* **41**:4277 (1990).
8. T. Naitoh, M. H. Ernst, and J. W. Dufty, *Phys. Rev. A* **42**:7187 (1990).
9. M. A. van der Hoef and D. Frenkel, *Physica D* **47**:191 (1991).
10. M. A. van der Hoef, M. Dijkstra, and D. Frenkel, *Europhys. Lett.* **17**:39 (1992).
11. T. Naitoh, M. H. Ernst, M. A. van der Hoef, and D. Frenkel, *Phys. Rev. A* **44**:24834 (1991).
12. T. Naitoh and M. H. Ernst, In *Proceeding Euromech Colloquium 267*, A. S. Alves, ed. (World Scientific, Singapore, 1991), p. 166.
13. J. J. Erpenbeck and W. W. Wood, *Phys. Rev. A* **26**:1648 (1982); **32**:412 (1985).
14. T. R. Kirkpatrick and M. H. Ernst, *Phys. Rev. A* **44**:8051 (1991).
15. R. Brito and M. H. Ernst, *Phys. Rev. A* **46**:875 (1992).
16. G. A. van Velzen, R. Brito, and M. H. Ernst, *J. Stat. Phys.* **70**:811 (1993).
17. M. H. Ernst and T. Naitoh, *J. Phys. A* **24**:2555 (1991).
18. M. H. Ernst and J. W. Dufty, *J. Stat. Phys.* **58**:57 (1990).
19. M. H. Ernst, *Liquids, Freezing and the Glass Transition, Les Houches, Session LI, 1989*, D. Levesque, J. P. Hansen, and J. Zinn-Justin, eds. (Elsevier, Amsterdam, 1991), p. 43.
20. Y. Pomeau and P. Résibois, *Phys. Rep.* **19**:64 (1975).
21. T. R. Wainwright, B. J. Alder, and D. M. Gass, *Phys. Rev. A* **4**:233 (1971).
22. M. A. van der Hoef and D. Frenkel, *Phys. Rev. Lett.* **66**:1591 (1991).
23. D. d'Humières and P. Lallemand, *Complex Syst.* **1**:599 (1987).
24. M. Gerits, M. H. Ernst, and D. Frenkel, *Phys. Rev. A* **48**:988 (1993).
25. B. J. Alder and W. E. Alley, *Phys. Today* **37**:56 (1984).
26. M. Henon, *Complex Syst.* **1**:475 (1987).
27. R. Brito and M. H. Ernst, *Phys. Rev. A* **44**:8384 (1991).